

# Chiral Perturbation Theory and the $pp \rightarrow pp\pi^0$ Reaction Near Threshold

T. Sato,<sup>a</sup> T.-S. H. Lee,<sup>b</sup> F. Myhrer<sup>c</sup> and K. Kubodera<sup>c</sup>

<sup>a</sup>*Department of Physics, Osaka University, Toyonaka, Osaka 560, Japan*

<sup>b</sup>*Physics Division, Argonne National Laboratory, Argonne, Illinois 60439-4843, U. S. A.*

<sup>c</sup>*Department of Physics and Astronomy, University of South Carolina*

*Columbia, SC 29208, U. S. A.*

## Abstract

A chiral-perturbative consideration of the near-threshold  $pp \rightarrow pp\pi^0$  reaction indicates that the pion-rescattering term has a substantial energy and momentum dependence. The existing calculations that incorporate this dependence give pion rescattering contributions significantly larger than those of the conventional treatment, and this enhanced rescattering term interferes destructively with the one-body impulse term, leading to theoretical cross sections that are much smaller than the observed values. However, since the existing calculations are based on coordinate-space representation, they involve a number of simplifying assumptions about the energy-momentum flow in the rescattering diagram, even though the delicate interplay between the one-body and two-body terms makes it desirable to avoid these kinematical assumptions. We carry out here a momentum-space calculation that retains the energy-momentum dependence of the vertices as predicted by chiral perturbation theory. Our improved treatment increases the rescattering amplitude by a factor of  $\sim 3$  over the value obtained in the r-space calculations. The  $pp \rightarrow pp\pi^0$  transition amplitude, which is now dominated by the rescattering

term, leads to the cross section much larger than what was reported in the approximate r-space calculations. Thus, the extremely small cross sections obtained in the previous chiral perturbative treatments of this reaction should be considered as an accidental consequence of the approximations employed rather than a general feature.

PACS numbers: 13.75.Cs, 13.75.Gx, 12.39.Fe

## I. INTRODUCTION

The high-precision measurements [1,2] of the total cross sections near threshold for the  $pp \rightarrow pp\pi^0$  reaction have invited many theoretical investigations on this process [3]- [9]. The pion production near threshold is expected to occur via the single-nucleon process (the impulse or Born term), Fig.1(a), and the  $s$ -wave pion rescattering process, Fig.1(b). In the conventional treatment [10], the  $\pi$ - $N$  vertex for the impulse term is assumed to be given by the Hamiltonian

$$\mathcal{H}_0 = \frac{g_A}{2f_\pi} \bar{\psi} \left( \vec{\sigma} \cdot \vec{\nabla} (\boldsymbol{\tau} \cdot \boldsymbol{\pi}) - \frac{i}{2m_N} \{ \vec{\sigma} \cdot \vec{\nabla}, \boldsymbol{\tau} \cdot \dot{\boldsymbol{\pi}} \} \right) \psi, \quad (1)$$

where  $g_A$  is the axial coupling constant, and  $f_\pi = 93$  MeV is the pion decay constant. The first term gives  $p$ -wave pion-nucleon coupling, while the second term accounts for the nucleon recoil effect. The  $s$ -wave rescattering vertex in Fig.1(b) is customarily described with the phenomenological Hamiltonian [10]

$$\mathcal{H}_1 = 4\pi \frac{\lambda_1}{m_\pi} \bar{\psi} \boldsymbol{\pi} \cdot \boldsymbol{\pi} \psi + 4\pi \frac{\lambda_2}{m_\pi^2} \bar{\psi} \boldsymbol{\tau} \cdot \boldsymbol{\pi} \times \dot{\boldsymbol{\pi}} \psi \quad (2)$$

The coupling constants  $\lambda_1$  and  $\lambda_2$  determined from the experimental pion-nucleon scattering lengths are  $\lambda_1 \sim 0.005$  and  $\lambda_2 \sim 0.05$ . Thus,  $\lambda_1 \ll \lambda_2$ , as expected from current algebra. The calculations [3,10] based on these phenomenological vertices yield cross sections for  $s$ -wave  $\pi^0$  production that are significantly smaller, typically by a factor of  $\sim 5$ , than the experimental

values [1]. There are, however, some delicate aspects in the calculated cross section. First, in Eq.(1), only the second term contributes to  $s$ -wave pion production. The suppression factor  $\sim m_\pi/m_N$  contained in this term drastically reduces the contribution of the impulse term, Fig.1(a), and as a consequence the relative importance of the two-body rescattering process, Fig.1(b), is enhanced. However, the dominant  $\lambda_2$  term in Eq.(2) cannot contribute to the  $pp\pi^0\pi^0$  vertex in Fig.1(b) due to its isospin structure. Thus, a phenomenological calculation based on Eqs.(1) and (2) leads to highly suppressed cross sections.

To describe the more recent theoretical developments, it is convenient to introduce what we call the *typical threshold (TT) kinematics*. Consider Fig.1(b) in the center of mass (CM) system with the initial and final interactions turned off. At threshold,  $(q_0, \vec{q}) = (m_\pi, \vec{0})$ ,  $p'_{10} = p'_{20} = m_N$ ,  $\vec{p}'_1 = \vec{p}'_2 = \vec{0}$ , so that  $p_{10} = p_{20} = m_N + m_\pi/2$ ,  $k_0 = m_\pi/2$ ,  $\vec{p}_1 = \vec{k} = -\vec{p}_2$  with  $|\vec{k}| = \sqrt{m_\pi m_N + m_\pi^2/4}$ . Needless to say, even for  $\vec{q} = 0$ , the actual kinematics for the transition process may differ from the *TT kinematics* due to the initial- and final-state interactions. Now, for the *TT kinematics* we have  $k^2 = -m_N m_\pi$ , which implies that the rescattering process typically probes inter-nucleon distances  $\sim 0.5$  fm. The reaction can therefore be sensitive to exchange of the heavy mesons, which play an important role in the phenomenological meson-exchange  $N$ - $N$  potentials. Lee and Riska [4] pointed out that the shorter-range meson exchanges were indeed capable of enhancing the cross section significantly. Meanwhile, even though the *off-shell*  $\pi N$  amplitudes feature in the rescattering process (*e.g.*,  $k^2 = -m_N m_\pi \neq m_\pi^2$  for the *TT kinematics*), there is no guarantee that  $\mathcal{H}_1$  of Eq.(2) describes the off-shell amplitudes adequately. Hernández and Oset [5] suggested that the  $s$ -wave amplitude enhanced for off-shell kinematics could increase the rescattering contribution sufficiently to reproduce the experimental cross sections. However, Ref. [5] used phenomenological off-shell extrapolations, the reliability of which requires further examination.

Chiral perturbation theory ( $\chi$ PT) [11,12] serves as a consistent framework to describe the low-energy  $\pi N$  scattering amplitudes. Taking advantage of this fact, Park *et al.* [7] (to be referred to as PM<sup>3</sup>K) and Cohen *et al.* [8] carried out the first  $\chi$ PT calculations for the

$pp \rightarrow pp\pi^0$  reaction. The results of these two groups [7,8] essentially agree with each other on the following major points: (1) the pion rescattering term in a  $\chi$ PT treatment is significantly larger than in the conventional treatment; (2) the sign of the rescattering term in a  $\chi$ PT treatment is opposite to that obtained in the conventional approach; (3) the enhanced rescattering term in a  $\chi$ PT treatment almost cancels the impulse term, leading to theoretical cross sections much smaller than the observed values. Thus a systematic treatment of the off-shell  $\pi N$  scattering amplitudes indeed drastically changes the  $pp \rightarrow pp\pi^0$  cross section. We note, however, that the calculations in Refs. [7,8], which rely on coordinate space representation, involve potentially problematic approximations on the kinematical variables appearing in the energy-dependent  $\pi N$  scattering amplitudes. Namely, in deriving the r-space representation of the two-body transition operator [see Fig. 1(b)], one limits oneself to the Feynman amplitude corresponding to the  $TT$  kinematics and Fourier-transforms it with respect to  $\vec{p}_1, \vec{p}_2, \vec{p}'_1$  and  $\vec{p}'_2$ , while keeping all the other kinematical variables fixed at their  $TT$  kinematics values. Although this type of simplification of kinematics is commonly used in nuclear physics to derive effective r-space operators, it is expected to be much less reliable for the threshold  $pp \rightarrow pp\pi^0$  reaction. The reason is two-fold: First, the energy-momentum exchange due to the initial and final-state interactions is vitally important for this process. Secondly, the destructive interference between the one-body and two-body terms implies that even a small change in the two-body term can influence the cross sections significantly.<sup>1</sup> In this article we carry out a  $\chi$ PT calculation for the  $pp \rightarrow pp\pi^0$  reaction with the use of momentum representation, which liberates us from the above-mentioned kinematical simplifications. As we shall show, this improvement drastically changes the calculated cross section.

This paper is organized as follows. We describe in section II the effective Lagrangian of

---

<sup>1</sup>A detailed momentum-space calculation by Hanhart *et al.* [6], with the use of the conventional Hamiltonian, indicates the importance of lifting the kinematical simplifications discussed here.

$\chi$ PT and a formalism we use to apply  $\chi$ PT to processes involving two or more nucleons. The details of our momentum-space calculation are explained in section III. In section IV we present the numerical results and comment on their salient features. The final section V contains discussion and concluding remarks.

## II. NUCLEAR CHIRAL PERTURBATION THEORY

As in PM<sup>3</sup>K [7], we use the heavy-fermion formalism (HFF) of chiral perturbation theory [13]. The effective Lagrangian  $\mathcal{L}_{\text{ch}}$  in the HFF is expanded as

$$\mathcal{L}_{\text{ch}} = \mathcal{L}^{(0)} + \mathcal{L}^{(1)} + \mathcal{L}^{(2)} + \dots \quad (3)$$

$\mathcal{L}^{(\bar{\nu})}$  represents a term of chiral order  $\bar{\nu}$  with  $\bar{\nu} \equiv d + (n/2) - 2$ , where  $n$  is the number of fermion lines involved in a vertex, and  $d$  is the number of derivatives or powers of  $m_\pi$ . In order to produce the one-body and two-body diagrams depicted in Figs.1(a) and 1(b), we minimally need terms with  $\bar{\nu} = 0$  and 1 [7]. Their explicit forms are [12]

$$\mathcal{L}^{(0)} = \frac{f_\pi^2}{4} \text{Tr}[\partial_\mu U^\dagger \partial^\mu U + m_\pi^2 (U^\dagger + U - 2)] + \bar{N}(iv \cdot D + g_A S \cdot u)N \quad (4)$$

$$\begin{aligned} \mathcal{L}^{(1)} = & -\frac{ig_A}{2m_N} \bar{N}\{S \cdot D, v \cdot u\}N + 2c_1 m_\pi^2 \bar{N}N \text{Tr}(U + U^\dagger - 2) \\ & + (c_2 - \frac{g_A^2}{8m_N}) \bar{N}(v \cdot u)^2 N + c_3 \bar{N}u \cdot uN \end{aligned} \quad (5)$$

We have retained here only terms of direct relevance for our present calculation. In the above,  $U(x)$  is an SU(2) matrix that is non-linearly related to the pion field and that has standard chiral transformation properties. We use  $U(x) = \sqrt{1 - [\boldsymbol{\pi}(x)/f_\pi]^2} + i\boldsymbol{\tau} \cdot \boldsymbol{\pi}(x)/f_\pi$  as in Ref. [12]. The large component of the heavy-fermion field is denoted by  $N(x)$ ; the four-velocity parameter  $v_\mu$  is chosen to be  $v_\mu = (1, 0, 0, 0)$ ;  $D_\mu N$  is the covariant derivative;  $S_\mu$  is the covariant spin operator and  $u_\mu = i[\xi^\dagger \partial_\mu \xi - \xi \partial_\mu \xi^\dagger]$ , where  $\xi = \sqrt{U(x)}$  [12]. The constants  $c_1, c_2$  and  $c_3$  have been determined from phenomenology [7,12] and their numerical values will be discussed later. In practical calculations,  $U(x)$  is expanded in powers of  $\boldsymbol{\pi}(x)/f_\pi$  and only necessary lowest order terms of this expansion are kept.

In applying  $\chi$ PT to nuclei [14], one classifies multi-nucleon Feynman diagrams into irreducible and reducible diagrams. Diagrams in which every intermediate state contains at least one meson are categorized as irreducible diagrams, and all others are classified as reducible diagrams. To each irreducible diagram one assigns the chiral order index  $\nu$  defined by  $\nu = 4 - E_N - 2C + 2L + \sum_i \bar{\nu}_i$ , where  $E_N$  is the number of nucleons in the Feynman diagram,  $L$  the number of loops,  $C$  the number of disconnected parts of the diagram, and the sum runs over all the vertices in the Feynman graph [14]. It can be shown that an irreducible diagram of order  $\nu$  carries a factor  $(q/\Lambda)^\nu$ , where  $q$  is a generic momentum characterizing low-energy phenomena and  $\Lambda \sim 1$  GeV is the scale parameter of  $\chi$ PT. This leads to the general expectation that the contributions of terms with higher values of  $\nu$  are significantly suppressed in the low-energy regime. Now, the contribution of all the irreducible diagrams (up to a specified chiral order) is treated as an effective operator  $\mathcal{T}$  acting on nucleonic wave functions. The resulting nuclear matrix elements incorporate the contributions of the reducible diagrams. This two-step procedure may be referred to as *nuclear chiral perturbation theory*.

Applying nuclear  $\chi$ PT to the present case, we write the transition amplitude for the  $pp \rightarrow pp\pi^0$  reaction as

$$T = \langle \Phi_f | \mathcal{T} | \Phi_i \rangle, \quad (6)$$

where  $|\Phi_i\rangle$  ( $|\Phi_f\rangle$ ) is the initial (final) two-nucleon state distorted by the initial-state (final-state) interaction. For formal consistency, if  $\mathcal{T}$  is calculated up to order  $\nu$ , the nucleon-nucleon interactions that generate  $|\Phi_i\rangle$  and  $|\Phi_f\rangle$  should also be calculated by summing up all irreducible two-nucleon scattering diagrams up to order  $\nu$ . In practice, however, it is common to use the phenomenological  $N$ - $N$  interactions that reproduce measured two-nucleon observables. This hybrid version of nuclear  $\chi$ PT has been applied with great success to electroweak transition processes [15], and we shall use this phenomenological version in this paper.

As discussed in PM<sup>3</sup>K, the lowest-order contributions to the impulse and rescattering

terms come from the  $\nu = -1$  and  $\nu = 1$  terms, respectively. With the use of  $\mathcal{L}_{\text{ch}}$  in Eq.(3), the matrix elements in momentum space<sup>2</sup> of these two terms are given by

$$\mathcal{T}^{(-1)} = \frac{i}{(2\pi)^{3/2}} \frac{1}{\sqrt{2\omega_q}} \frac{g_A}{2f_\pi} \sum_{j=1,2} [-\vec{\sigma}_j \cdot \vec{q} + \frac{\omega_q}{2m_N} \vec{\sigma}_j \cdot (\vec{p}_j + \vec{p}'_j)] \tau_j^0, \quad (7)$$

$$\mathcal{T}^{(+1)} = \frac{-i}{(2\pi)^{9/2}} \frac{1}{\sqrt{2\omega_q}} \frac{g_A}{f_\pi} \sum_{j=1,2} \kappa(k_j, q) \frac{\vec{\sigma}_j \cdot \vec{k}_j \tau_j^0}{k_j^2 - m_\pi^2}, \quad (8)$$

where  $\vec{p}_j$  and  $\vec{p}'_j$  ( $j = 1, 2$ ) denote the initial and final momenta of the  $j$ -th proton. The four-momentum of the exchanged pion is defined by the nucleon four-momenta at the  $\pi NN$  vertex:  $k_j \equiv p_j - p'_j$ , where  $p_j = (E_{p_j}, \vec{p}_j)$ ,  $p'_j = (E_{p'_j}, \vec{p}'_j)$  with the definition  $E_p = (\vec{p}^2 + m_N^2)^{1/2}$ . The rescattering vertex function  $\kappa(k, q)$  is calculated from Eq.(5):

$$\kappa(k, q) \equiv \frac{m_\pi^2}{f_\pi^2} \left[ 2c_1 - \left( c_2 - \frac{g_A^2}{8m_N} \right) \frac{\omega_q k_0}{m_\pi^2} - c_3 \frac{q \cdot k}{m_\pi^2} \right], \quad (9)$$

where  $k = (k_0, \vec{k})$  and  $q = (\omega_q, \vec{q})$  represent the four-momenta of the exchanged and final pions, respectively. The time component of the final pion is obviously defined by  $\omega_q = (\vec{q}^2 + m_\pi^2)^{1/2}$ .

In what follows, we work with  $\mathcal{T}$  defined by

$$\mathcal{T} = \mathcal{T}^{(-1)} + \mathcal{T}^{(+1)} \equiv \mathcal{T}^{\text{Imp}} + \mathcal{T}^{\text{Resc}} \quad (10)$$

To specify the transition operator  $\mathcal{T}$  completely, we need the values of the low-energy coefficients  $c_1$ ,  $c_2$  and  $c_3$ . In Ref. [12], these parameters were determined from the experimental values of the pion-nucleon  $\sigma$  term, the nucleon axial polarizability  $\alpha_A$  and the isospin-even s-wave  $\pi N$  scattering length  $a^+$ . The results are

$$c_1 = -0.87 \pm 0.11 \text{ GeV}^{-1}, \quad c_2 = 3.34 \pm 0.27 \text{ GeV}^{-1}, \quad c_3 = -5.25 \pm 0.22 \text{ GeV}^{-1}. \quad (11)$$

As discussed in PM<sup>3</sup>K, the value of  $c_2 + c_3$  can also be extracted from the known pion-nucleon effective range parameter  $b^+$  of the low energy pion-nucleon scattering amplitude:

---

<sup>2</sup>Here we normalize plane-wave states according to  $\langle \vec{p}' | \vec{p} \rangle = \delta(\vec{p}' - \vec{p})$ ; this normalization differs from the one used in Ref. [7].

$$b^+ = \frac{1}{2\pi} \left(1 + \frac{m_\pi}{m_N}\right)^{-1} \left(\frac{m_\pi}{f_\pi}\right)^2 (c_2 + c_3 - \frac{g_A^2}{8m_N}) \frac{1}{m_\pi^2}. \quad (12)$$

Since  $c_3$  in Eq. (11) has been deduced directly from  $\alpha_A^{\text{exp}}$ , a quantity known with a relatively high precision, we may use the value of  $c_3$  in Eq. (11) to determine  $c_2$  from the observed value of  $b^+$ . This procedure yields  $c_2 = (4.5 \pm 0.7) \text{ GeV}^{-1}$  [7], which is significantly larger than that in Eq.(11). Thus, the errors quoted in Eq.(11) do not seem to reflect the entire range of uncertainties in the low-energy coefficients.<sup>3</sup> It is important to examine to what extent the existing ambiguities in the low-energy coefficients affect the off-shell enhancement of the  $pp \rightarrow pp\pi^0$  reaction. In the present work, we use as the “standard” parameter set the central values in Eq. (11) and refer to it as the parameter set I. We also use the parameter set II, in which the value of  $c_2$  is changed into  $c_2 = 4.5 \text{ GeV}^{-1}$ . Furthermore, in developing a certain argument later in the text, we shall be interested in the lower end of the error bars in the empirical  $c_1$ . For this we introduce the parameter set III, which is identical to the set I except the change:  $c_1 = -0.87 \text{ GeV}^{-1} \rightarrow c_1 = (-0.87 - 0.11) \text{ GeV}^{-1} = -0.98 \text{ GeV}^{-1}$ . Thus, we will consider three sets of low-energy coefficients:

Parameter set I

$$c_1 = -0.87 \text{ GeV}^{-1}, \quad c_2 = 3.34 \text{ GeV}^{-1}, \quad c_3 = -5.25 \text{ GeV}^{-1} \quad (13)$$

Parameter set II

$$c_1 = -0.87 \text{ GeV}^{-1}, \quad c_2 = 4.5 \text{ GeV}^{-1}, \quad c_3 = -5.25 \text{ GeV}^{-1} \quad (14)$$

Parameter set III

$$c_1 = -0.98 \text{ GeV}^{-1}, \quad c_2 = 3.34 \text{ GeV}^{-1}, \quad c_3 = -5.25 \text{ GeV}^{-1} \quad (15)$$

Before embarking on numerical work we make two remarks. First,  $\mathcal{T}^{(+1)}$  above represents only the tree-diagram contribution, Fig.1(b); loop corrections to the  $\nu = -1$  impulse term

---

<sup>3</sup> In this connection, it is worth mentioning that the reliability of the empirical value of the  $s$ -wave  $\pi N$  scattering length  $a^+$  has recently been questioned [16].



generate transition operators of order  $\nu = 1$ . These additional contributions generate an effective  $\pi NN$  vertex form factor for the impulse term, Fig.1(a), but according to PM<sup>3</sup>K's estimate, the net effect of the loop corrections after renormalization is less than 20% of the leading-order impulse term. We therefore neglect the loop corrections in the present work, even though formal consistency requires it. We will return to this question in later work. Secondly, the nuclear chiral counting procedure employed above is in fact best applicable when energy-momentum transfers to a nucleus are small, whereas the near-threshold  $pp \rightarrow pp\pi^0$  reaction involves significant energy transfers  $q_0 \sim m_\pi$ . Hence we must exercise caution in applying Weinberg's counting rule to this reaction. In PM<sup>3</sup>K, as far as the construction of the transition operators was concerned, the energy-momentum transfer due to the final pion was ignored (*i.e.*, the external pion was taken to be soft,  $q_\mu \approx 0$ ) in order to utilize Weinberg's original counting rule. The physical value of  $q_\mu$  was used only at the stage of calculating the phase space integral. The approximate nature of this method is particularly evident for the impulse term, where the pion-emitting nucleon is off-shell by  $\sim m_\pi$ . This off-shell nucleon must interact at least once with the second nucleon before losing its off-shell character. It is then sensible to treat an impulse diagram accompanied by subsequent one-pion exchange as an irreducible diagram, even though the original Weinberg classification would categorize it as a reducible diagram. Cohen *et al.* [8] proposed a modified chiral counting rule that takes account of this feature. In addition, these authors argued that the  $\Delta$  degree of freedom should be taken into account explicitly in  $\chi$ PT since the  $N$ - $\Delta$  mass difference  $\sim 2m_\pi$  is small on the chiral scale  $\Lambda$  (see also Ref. [17]). In the present work, which is basically of the illustrative nature, we do not address these issues but simply use the transition operator given in Eq. (10) with the view to concentrating on the pragmatic (but in our opinion very urgent) question: For a *given* version of  $\chi$ PT transition operators, how important is the difference between the conventional r-space calculation and a p-space calculation ?

### III. NUMERICAL CALCULATIONS

#### A. Momentum space calculation

It is most convenient to carry out the calculation in the CM frame. Referring to Fig. 1, we denote by  $\vec{p}$  and  $\vec{p}'$  the relative momenta of the two protons before and after the pion emission, respectively. In terms of  $\vec{p}$ ,  $\vec{p}'$  and the momentum of the final pion  $\vec{q}$ , the momentum of each nucleon in Fig. 1 is written as

$$\vec{p}_1 = -\vec{p}_2 = \vec{p}, \quad \vec{p}'_1 = \vec{p}' - \frac{\vec{q}}{2}, \quad \vec{p}'_2 = -\vec{p}' - \frac{\vec{q}}{2}. \quad (16)$$

With the normalization of plane-wave states specified earlier, the plane-wave matrix element of the production operator defined by Eqs. (7)-(10) takes the following form

$$\langle \vec{p}', \vec{q} | \mathcal{T} | \vec{p} \rangle = \langle \vec{p}', \vec{q} | \mathcal{T}^{\text{Imp}} | \vec{p} \rangle + \langle \vec{p}', \vec{q} | \mathcal{T}^{\text{Resc}} | \vec{p} \rangle, \quad (17)$$

where

$$\begin{aligned} \langle \vec{p}', \vec{q} | \mathcal{T}^{\text{Imp}} | \vec{p} \rangle &= \frac{i}{(2\pi)^{3/2}} \frac{1}{\sqrt{2\omega_q}} \frac{g_A}{2f_\pi} \left[ -\vec{\sigma}_1 \cdot \vec{q} + \frac{\omega_q}{2m_N} \vec{\sigma}_1 \cdot (\vec{p}_1 + \vec{p}'_1) \right] \delta(\vec{p}_2 - \vec{p}'_2) \\ &\quad + [1 \leftrightarrow 2] \end{aligned} \quad (18)$$

and

$$\langle \vec{p}', \vec{q} | \mathcal{T}^{\text{Resc}} | \vec{p} \rangle = \frac{-i}{(2\pi)^{9/2}} \frac{1}{\sqrt{2\omega_q}} \frac{g_A}{f_\pi} \frac{\kappa(k_1, q) \vec{\sigma}_1 \cdot \vec{k}_1}{k_1^2 - m_\pi^2} + [1 \leftrightarrow 2]. \quad (19)$$

In the above, the four-momentum transfer  $k_j$  ( $j = 1, 2$ ) is defined by  $k_j = (E_{\vec{p}_j} - E_{\vec{p}'_j}, \vec{p}_j - \vec{p}'_j)$  with  $E_{\vec{p}_j} = (\vec{p}_j^2 + m_N^2)^{1/2}$ . Since we are assuming that the nuclear states are described by the non-relativistic Schrödinger equation, the  $N$ - $N$  potential responsible for the initial- and final-state interactions represents only those two-nucleon diagrams that involve no energy transfer between the two nucleons (*i.e.*, three-momentum transfers only). Hence the intermediate nucleon energies in our treatment are given by  $E_{\vec{p}_j} = (\vec{p}_j^2 + m_N^2)^{1/2}$  at each pion-nucleon vertex.

The transition amplitude of the  $pp \rightarrow pp\pi^0$  reaction is evaluated by taking the matrix element of the production operator  $\mathcal{T}$  defined above between the initial ( $\chi^{(+)}$ ) and the final ( $\chi^{(-)}$ )  $pp$  scattering wavefunctions. In terms of this transition matrix element, the total cross section is given by

$$\begin{aligned} \sigma_{pp \rightarrow pp\pi^0}(W) &= \frac{(2\pi)^4}{2v_i} \int d\vec{p}_f d\vec{q} \delta(\sqrt{4E_{\vec{p}_f}^2 + \vec{q}^2} + \omega_q - W) \\ &\times \frac{1}{4} \sum_{m_{s_1} m_{s_2} m_{s'_1} m_{s'_2}} |\langle \chi_{\vec{p}_f, m_{s'_1}, m_{s'_2}}^{(-)}, \vec{q} | \mathcal{T} | \chi_{\vec{p}_i, m_{s_1}, m_{s_2}}^{(+)} \rangle|^2, \end{aligned} \quad (20)$$

where  $\vec{p}_i$  and  $\vec{p}_f$  are the *asymptotic* relative momenta of the initial and final  $pp$  states, respectively,  $W = 2E_{\vec{p}_i}$  is the total energy,  $v_i = 2|\vec{p}_i|/E_{\vec{p}_i}$  is the asymptotic relative velocity of the two initial protons, and  $m_{s_j}$  is the z-component of the spin of the  $j$ th nucleon. Eq.(20) can be calculated most easily in the partial-wave representation. We therefore expand the transition matrix element as

$$\begin{aligned} \langle \chi_{\vec{p}_f, m_{s'_1}, m_{s'_2}}^{(-)}, \vec{q} | \mathcal{T} | \chi_{\vec{p}_i, m_{s_1}, m_{s_2}}^{(+)} \rangle &= \\ &\sum_{S_f L_f J_f M_f} \sum_{S_i L_i J_i M_i} \mathcal{Y}_{S_f L_f}^{J_f M_f}(\hat{p}_f, m_{s'_1}, m_{s'_2}) \mathcal{Y}_{S_i L_i}^{J_i M_i}(\hat{p}_i, m_{s_1}, m_{s_2}) \\ &\times \sum_{l_\pi m_\pi} Y_{l_\pi m_\pi}^*(\hat{q}) \langle p_f [L_f S_f] J_f M_f | \mathcal{T}_{l_\pi m_\pi}(q) | p_i [L_i S_i] J_i M_i \rangle, \end{aligned} \quad (21)$$

where the spin-angular function of the anti-symmetrized two proton state is defined by

$$\begin{aligned} \mathcal{Y}_{LS}^{JM}(\hat{p}, m_{s_1}, m_{s_2}) &= \sum_{m_{s_1} m_{s_2}} \frac{1 - (-1)^{L+S+1}}{\sqrt{2}} \sum_{M_S M_L} i^L e^{i\delta_{(LS)J}} Y_{LM_L}^* Y_{LM_S}(\hat{p}) \\ &\times \langle \frac{1}{2} m_{s_1} m_{s_2} | S M_S \rangle \langle L S M_L M_S | J M \rangle, \end{aligned} \quad (22)$$

where  $\delta_{(LS)J}$  is the NN scattering phase shift in the eigenchannel defined by the orbital angular momentum  $L$ , total spin  $S$ , and total angular momentum  $J$ . We introduce the reduced matrix element using the standard convention:

$$\begin{aligned} \langle p_f [L_f S_f] J_f M_f | \mathcal{T}_{l_\pi m_\pi}(q) | p_i [L_i S_i] J_i M_i \rangle &\equiv \\ (-1)^{J_f - M_f} \begin{pmatrix} J_f & l_\pi & J_i \\ -M_f & m_\pi & M_i \end{pmatrix} \langle p_f [L_f S_f] J_f || T_{l_\pi}(q) || p_i [L_i S_i] J_i \rangle. \end{aligned} \quad (23)$$

The substitution of Eqs. (21)-(23) into Eq.(20) leads to

$$\begin{aligned} \sigma_{pp \rightarrow pp\pi^0}(W) &= \frac{(2\pi)^4 E_{p_i}}{16 p_i} \int_0^{q_m} dq q^2 p_f \sqrt{4E_{p_f}^2 + \vec{q}^2} \\ &\times \sum_{L_i S_i J_i L_f S_f J_f l_\pi} \left| \frac{1}{\sqrt{4\pi}} e^{i\delta(L_f S_f)J_f + i\delta(L_i S_i)J_i} \langle p_f [L_f S_f] J_f || \mathcal{T}_{l_\pi}(q) || p_i [L_i S_i] J_i \rangle \right|^2 \end{aligned} \quad (24)$$

where  $E_{p_f} \equiv \{(W - \omega_q)^2 - \vec{q}^2\}^{1/2}/2$ ,  $p_f \equiv \sqrt{E_{p_f}^2 - m_N^2}$ , and the maximum momentum of the pion is given by  $q_m = \sqrt{\{(W - 2m_N)^2 - m_\pi^2\}\{(W + 2m_N)^2 - m_\pi^2\}/4W^2}$ . Corresponding to the decomposition  $\mathcal{T} = \mathcal{T}^{\text{Imp}} + \mathcal{T}^{\text{Resc}}$  in Eq. (17), we have

$$\begin{aligned} &\langle p_f [L_f S_f] J_f || \mathcal{T}_{l_\pi}(q) || p_i [L_i S_i] J_i \rangle \\ &= \langle p_f [L_f S_f] J_f || \mathcal{T}_{l_\pi}^{\text{Imp}}(q) || p_i [L_i S_i] J_i \rangle + \langle p_f [L_f S_f] J_f || \mathcal{T}_{l_\pi}^{\text{Resc}}(q) || p_i [L_i S_i] J_i \rangle, \end{aligned} \quad (25)$$

where each of the reduced matrix elements on the right-hand side is defined similarly to Eq. (23).

For the near-threshold  $\pi$  production under consideration, we limit ourselves to the case where the produced pion is in s-wave ( $l_\pi = 0$ ) and the final  $pp$  state is in the  $^1S_0$  state. Accordingly, the initial  $pp$  state is restricted to be in the  $^3P_0$  state.

Computation of the reduced matrix elements in Eq. (25) involves only the radial parts of the scattering wavefunctions. We calculate the momentum-space radial wavefunction from the half-off-shell  $K$ -matrix

$$R_{(LS)J,p_0}(p) = i^{-L} \cos(\delta_{(LS)J}) \left[ \frac{\delta(p - p_0)}{p_0^2} + \mathcal{P} \frac{K_{(LS)J}(p, p_0, W)}{p_0^2/m_N - p^2/m_N} \right] \quad (26)$$

where  $\mathcal{P}$  means taking the principal-value part of the two-nucleon propagator, and  $p_0$  is the on-shell momentum defined by  $W = 2E_{p_0}$ . The  $K$ -matrix is related to the phase shift by  $\rho K_{(LS)J}(p_0, p_0, W) = -\tan(\delta_{(LS)J})$  with  $\rho = \pi p_0 m_N/2$ . By using the well-developed numerical methods (see, *e.g.*, Ref. [18]), the  $K$ -matrix (or the scattering t-matrix) can be calculated directly from the potential by solving the Lippman-Schwinger equation in momentum space. In terms of these radial functions, the reduced matrix element for the impulse term is written as

$$\begin{aligned} \frac{1}{\sqrt{4\pi}} \langle p_f [^1S_0] || \mathcal{T}_{l_\pi}^{\text{Imp}}(q) || p_i [^3P_0] \rangle &= \frac{-i}{\sqrt{(2\pi)^3 2\omega_q}} \frac{g_A}{f_\pi} \int \int \frac{d\vec{p}' d\vec{p}}{4\pi} R_{1S_0, p_f}(p') \\ &\times \hat{p} \cdot \left(-\vec{q} + \frac{\omega_q}{m_N} \vec{p}'\right) \delta(\vec{p}' - \vec{p} + \vec{q}/2) R_{3P_0, p_i}(p) \end{aligned} \quad (27)$$

while the reduced matrix element of the rescattering term is given by

$$\begin{aligned} \frac{1}{\sqrt{4\pi}} \langle p_f [^1S_0] || \mathcal{T}_{l_\pi=0}^{\text{Resc}}(q) || p_i [^3P_0] \rangle &= \frac{i}{\sqrt{(2\pi)^3 2\omega_q}} \frac{2g_A}{f_\pi} \int \int \frac{d\vec{p}' d\vec{p}}{4\pi} R_{1S_0, p_f}(p') \\ &\times \frac{\kappa(k, q)}{(2\pi)^3} \frac{\hat{p} \cdot \vec{k}}{k^2 - m_\pi^2} R_{3P_0, p_i}(p) \end{aligned} \quad (28)$$

where  $k = (k_0, \vec{k}) = (E_{\vec{p}} - E_{\vec{p}' - \vec{q}/2}, \vec{p} - \vec{p}' + \vec{q}/2)$ . As will be discussed in the next subsection, an accurate numerical calculation of the impulse term Eq.(27) is possible either in momentum space or in coordinate space. By contrast, since the rescattering term Eq.(28) is highly nonlocal, its accurate numerical calculation is possible only in momentum space.

## B. Expressions in r-space

We now relate our p-space calculation to the r-space calculations in the literature. With the use of the usual normalization  $\langle \vec{r} | \vec{r}' \rangle = \delta(\vec{r} - \vec{r}')$  for the r-space base vectors, the radial functions in p- and r-space are related to each other by the standard Bessel transformation

$$R_{(LS)J, p_0}(r) = \sqrt{\frac{2}{\pi}} i^L \int p^2 dp j_L(pr) R_{(LS)J, p_0}(p), \quad (29)$$

and  $R_{(LS)J, p_0}(r)$  satisfies the boundary condition

$$R_{(LS)J, p_0}(r) \xrightarrow{r \rightarrow \infty} \sqrt{\frac{2}{\pi}} [\cos(\delta_{(LS)J}) j_L(p_0 r) - \sin(\delta_{(LS)J}) n_L(p_0 r)], \quad (30)$$

where  $j_L(x)$  and  $n_L(x)$  are the regular and irregular spherical Bessel functions.

As for the impulse term, the momentum-space expression, Eq. (27), can be easily cast into the coordinate-space expression with the use of Eq. (29). The result is

$$\begin{aligned} \frac{1}{\sqrt{4\pi}} \langle p_f [^1S_0] || \mathcal{T}_{l_\pi=0}^{\text{Imp}}(q) || p_i [^3P_0] \rangle &= \frac{1}{\sqrt{(2\pi)^3 2\omega_q}} \frac{g_A}{f_\pi} \int dr r^2 R_{1S_0, p_f}(r) \\ &\times \left[ \left(1 + \frac{\omega_q}{2m_N}\right) q j_1(qr/2) \right. \\ &\left. - \frac{\omega_q}{m_N} j_0(qr/2) \left(\frac{d}{dr} + \frac{2}{r}\right) \right] R_{3P_0, p_i}(r) \end{aligned} \quad (31)$$

In the  $\vec{q} \rightarrow 0$  limit, this expression reduces to

$$\frac{1}{\sqrt{4\pi}} \langle p_f [^1S_0] || \mathcal{T}_{l_\pi=0}^{\text{Imp}} || p_i [^3P_0] \rangle_{\vec{q} \rightarrow 0} = \frac{-1}{\sqrt{(2\pi)^3 2m_\pi}} \times \frac{g_A m_\pi}{f_\pi m_N} \int dr r^2 R_{1S_0, p_f}(r) \left( \frac{d}{dr} + \frac{2}{r} \right) R_{3P_0, p_i}(r), \quad (32)$$

and this corresponds to Eq. (54a) of PM<sup>3</sup>K.

As stated, the rescattering operator is highly non-local and hence its matrix element, Eq. (28), can be evaluated exactly only in momentum space. The relation between the full expression, Eq. (28), and the approximate r-space form used in the PM<sup>3</sup>K calculation is as follows. We first simplify Eq. (28) by taking the  $\vec{q} \rightarrow 0$  limit:

$$\frac{1}{\sqrt{4\pi}} \langle p_f [^1S_0] || \mathcal{T}_{l_\pi=0}^{\text{Resc}} || p_i [^3P_0] \rangle_{\vec{q} \rightarrow 0} = \frac{-2\pi i}{\sqrt{(2\pi)^3 2m_\pi}} \frac{g_A}{f_\pi} \int dp dp' pp' R_{1S_0, p_f}(p') \frac{\bar{\kappa}}{(2\pi)^3} \times \left\{ 2p' + (p - xp') \log \frac{x+1}{x-1} \right\} R_{3P_0, p_i}(p) \quad (33)$$

where

$$x \equiv \frac{p^2 + p'^2 - k_0^2 + m_\pi^2}{2pp'}, \quad k_0 = E_p - E_{p'}, \quad (34)$$

and  $\bar{\kappa}$  is defined [cf. Eq.(9)] as

$$\bar{\kappa} = \frac{m_\pi^2}{f_\pi^2} \left[ 2c_1 - \left( c_2 - \frac{g_A^2}{8m_N} + c_3 \right) \frac{k_0}{m_\pi} \right] \quad (35)$$

If we furthermore freeze  $k_0$ , the energy variable of the exchanged pion, at the *fixed* value  $k_0 = m_\pi/2$  corresponding to the threshold pion production, then we are back with the *TT kinematics* explained in section I. For the *TT kinematics*,

$$x \xrightarrow{k_0=m_\pi/2} \frac{p^2 + p'^2 + 3m_\pi^2/4}{2pp'}, \quad (36)$$

and  $\bar{\kappa}$  becomes a constant, which was denoted by  $\kappa_{th}$  in Eq. (32) of PM<sup>3</sup>K:

$$\bar{\kappa} \xrightarrow{k_0=m_\pi/2} \kappa_{th} \equiv \frac{m_\pi^2}{f_\pi^2} \left[ 2c_1 - \frac{1}{2} \left( c_2 - \frac{g_A^2}{8m_N} \right) - \frac{1}{2} c_3 \right] \quad (37)$$

We refer (as in PM<sup>3</sup>K) to the simplifications Eqs. (33), (36), (37) as the *fixed kinematics approximation*. In the *fixed kinematics approximation*, the right-hand side of Eq. (28) becomes sufficiently simple to be recast into an r-space expression via the transformation Eq.(29). The resulting expression agrees with the r-space form Eq.(54b) of PM<sup>3</sup>K.

#### IV. NUMERICAL RESULTS

To calculate the reduced matrix element  $\langle p_f[{}^1S_0] || \mathcal{T}_{l_\pi}^{\text{Imp}}(q) || p_i[{}^3P_0] \rangle$ , we can use either Eq.(27) or Eq.(31); these are completely equivalent to each other. For numerical computations, however, we find the latter more convenient. On the other hand, the reduced matrix element for the rescattering term,  $\langle p_f[{}^1S_0] || \mathcal{T}_{l_\pi=0}^{\text{Resc}}(q) || p_i[{}^3P_0] \rangle$ , is calculated with the use of the p-space expression, Eq.(28). Calculations that are based on the full expressions, Eq. (27)(or Eq. (31)) and Eq. (28) are referred to as *full p-space* calculations. For the sake of comparison, we also carry out calculations with the use of the approximate expressions discussed in the preceding section. For given reduced matrix elements, the total cross section is obtained via Eqs. (24), (25).

The radial functions for the  $pp$  scattering states that appear in Eqs. (28), (31) are to be generated with the use of realistic nucleon-nucleon interactions. We adopt here as our standard choice the Argonne V18 potential [19]. For the purpose of comparison, we also carry out supplementary calculations with the Reid soft-core potential [20]. As regards the low-energy coefficients,  $c_1$ ,  $c_2$  and  $c_3$ , our standard choice is the parameter set I [Eq. (13)], and we use it throughout unless otherwise stated.

We note here that the accuracy of the numerical integration for the rescattering term, Eq. (28), can be achieved only when the high momentum component of  $pp$  wavefunction is accounted for correctly. This is due to the fact that the  $c_2$  and  $c_3$  terms in  $\kappa(k, q)$ , Eq.(9), grow linearly with the momentum for higher momenta. We have found that a very large number of mesh points are needed to achieve sufficient numerical accuracies in evaluating the rescattering term.

Figs. 2 - 4 show the total cross sections calculated with the Argonne V18 potential and with the parameter set I. It is informative to first consider the behavior of the individual contributions of the impulse and rescattering terms and then proceed to discuss the behavior of their coherent sum. Figs. 2 and 3 give the individual contributions of the impulse and rescattering terms, respectively, while Fig. 4 presents the cross sections due to the coherent

sum of these two terms.

The cross sections in Fig. 2 have been obtained by retaining only the impulse term in the decomposition Eq. (25). The solid curve corresponds to the full calculation based on Eq. (31), while the broken line has been obtained with the  $\vec{q} \rightarrow 0$  approximation, Eq. (32). Our numerical results for the latter case coincide with those in PM<sup>3</sup>K. As expected, the  $\vec{q} = 0$  approximation employed in PM<sup>3</sup>K becomes less accurate as the collision energy increases. Although the difference between the two results is not extremely large as far as the isolated contribution of the impulse term is concerned, yet we should remember that, depending on the pattern of interference between the impulse and rescattering terms, even a rather minor change in the impulse contribution may affect the cross section significantly. It is therefore recommended to avoid the  $\vec{q} = 0$  approximation in computing the impulse term.

We next discuss the contribution of the rescattering term. Fig. 3 shows the cross sections obtained by retaining only the rescattering term in Eq. (25). The solid curve corresponds to the full p-space calculation. The dash-dotted curve gives the result obtained with the use of the approximation Eq. (33), in which  $\vec{q}$  is fixed to be zero while the energy-transfer  $k_0$  in the exchanged pion propagator and in the coefficient  $\kappa(k, q)$  is treated exactly. The dashed curve represents the results of the *fixed kinematics approximation*, viz.,  $\vec{q} \equiv 0$  and  $k_0 \equiv m_\pi/2$ ; our numerical results for this case reproduce those obtained in PM<sup>3</sup>K. The difference between the dash-dotted and dashed lines clearly indicates that the non-local effects due to the  $k_0$ -dependence enhance the cross sections by a very large factor. The smaller but still substantial difference between the solid and dash-dotted curve implies that the  $\vec{q}$ -dependence of the pion propagator and of the rescattering coupling coefficient  $\kappa$  cannot be neglected in a quantitative calculation of the  $pp \rightarrow pp\pi^0$  cross section. The solid curve and the dashed curve differ by a factor as large as  $\sim 10$ . Thus the magnitude of the rescattering amplitude obtained in the full p-space calculation is  $\sim 3$  times larger than that obtained in the *fixed kinematics approximation*. In Refs. [7,8], the impulse and rescattering terms gave transition amplitudes of about the same magnitude, and this feature is also visible in Figs. 2 and 3 (compare the dashed lines therein). In the full p-space calculation, however, it is



the rescattering term that is dominant, and this feature drastically changes the interference pattern of the two terms, as discussed immediately below.

In all the cases shown in Figs. 2 and 3, our numerical results indicate that the reduced matrix element for the impulse term  $\langle p_f[{}^1S_0] || \mathcal{T}_{l_\pi}^{\text{Imp}}(q) || p_i[{}^3P_0] \rangle$  and that for the rescattering term  $\langle p_f[{}^1S_0] || \mathcal{T}_{l_\pi=0}^{\text{Resc}}(q) || p_i[{}^3P_0] \rangle$  have opposite signs so that they interfere with each other destructively. The cross sections given by the coherent sum of these two terms are given in Fig. 4. The solid curve represents  $\sigma_{\text{full}}$ , the cross section obtained in the full p-space calculation. The dash-dotted curve corresponds to the approximation Eq. (33). The cross section  $\sigma_{\text{fix. kin.}}$  corresponding to the *fixed kinematics approximation*, if plotted in the same scale, would be hardly visible. The impulse and rescattering contributions in this case cancel each other almost perfectly, leading to an extremely small value of  $\sigma_{\text{fix. kin.}}$ . This is consistent with the previous r-space calculations [7,8]. To illustrate the calculated  $\sigma_{\text{fix. kin.}}$ , we multiply it by a factor of 30 to obtain the dashed curve in Fig.4. When the approximation  $k_0 = m_\pi/2$  is removed, the scattering term is substantially enhanced (see Fig. 2), and as a consequence there is only a partial cancellation between the impulse and rescattering terms. The corresponding cross section (dash-dotted curve) therefore becomes significantly larger than  $\sigma_{\text{fix. kin.}}$ . This tendency is even more prominent as we go to the full p-space calculation by removing the  $\vec{q} \rightarrow 0$  approximation; the solid line representing  $\sigma_{\text{full}}$  exhibits a huge enhancement over  $\sigma_{\text{fix. kin.}}$ .

The results in Fig. 4 indicate that the extremely small cross sections reported in Refs. [7,8] are an accidental consequence of the kinematical approximations used there rather than a general feature of calculations based on nuclear  $\chi PT$ . It is to be noted, however, that  $\sigma_{\text{full}}$  in the present calculation is still significantly smaller than the observed cross sections. Our calculation here does *not* include the Coulomb repulsion effect in the initial and final  $pp$  states. The inclusion of the Coulomb effect is expected to further reduce the cross section [3], worsening the discrepancy between the calculated and observed cross sections.

We have already mentioned that the results presented in Figs. 2-4 are obtained with the Argonne V18 potential and with the parameter set I, Eq.(13). To provide some measure of

the sensitivity of the cross section to input  $NN$  potentials, we have repeated a full p-space calculation with the use of the Reid soft-core potential [20], while retaining the parameter set I for the low-energy coefficients. The resulting cross section is given in Fig. 5 (dashed curve) along with the result for the Argonne V18 potential (solid curve). The difference between these two results is not significant.

To examine the sensitivity to different choices of the low-energy coefficients, we have carried out full p-space calculations, with the Argonne V18 potential, for the parameter set II, Eq. (14), and for the parameter set III, Eq. (15). The dashed curve in Fig. 6 represents the cross section corresponding to the parameter set II. This curve is almost indistinguishable from the solid curve obtained with the parameter set I even though these two sets have significantly different values of  $c_2$ . At first sight, this feature is puzzling because the large difference between  $\sigma_{\text{full}}$  and  $\sigma_{\text{fix. kin.}}$  seen in Fig. 4 seems to suggest that the cross sections should also be sensitive to the parameters contained in the vertex function  $\kappa(k, q)$ . On closer examination, however, the lack of sensitivity to  $c_2$  in the full p-space calculation has a simple explanation. In the near-threshold region ( $\vec{q} \rightarrow 0$ ) under consideration, the  $c_2$ - and  $c_3$ - terms in the vertex function  $\kappa(k, q)$ , Eq. (9), depend on a factor  $k_0 = E_p - E_{p'}$  [see also Eq. (35)]. This energy factor introduces a zero in the transition operator at  $|\vec{p}| = |\vec{p}'|$ , which drastically reduces the contributions from the  $c_2$ - and  $c_3$ -terms to the integration over the scattering wavefunctions. As a result, the rescattering term is dominated by the  $c_1$ -term in the full p-space calculation. In contrast, in the *fixed kinematics approximation* (see Eq.(37)), the transition operator arising from the  $c_2$ - and  $c_3$ -terms are momentum-independent and of comparable magnitude but of opposite sign to the transition operator coming from the  $c_1$ -term. This means a substantial cancellation between these two operators at all momenta and hence the rescattering transition matrix element can be a sensitive function of the low energy coefficients including  $c_2$  in the *fixed kinematics approximation* calculation. This feature originating from the treatment of  $k_0$  essentially accounts for the large difference (by a factor of  $\sim 3$ ), discussed earlier, between the rescattering amplitudes obtained in the full p-space calculation and in the *fixed kinematics approximation* (see the discussion on Fig. 3).

The same feature also explains why the cross section in the full treatment is hardly sensitive to  $c_2$  (and  $c_3$ ).

The dominance of the  $c_1$ -term in the full p-space calculations implies that the cross section should be sensitive to an input value of  $c_1$ , a coefficient linked to the pion-nucleon sigma term [12]. In Fig. 6 we compare the results of full p-space calculations corresponding to the parameter sets I and III, which differ only in the value of  $c_1$ . The cross sections indeed vary substantially as we change the value of  $c_1$  from the currently accepted central value to one end of the error bars [see Eq. (11)]. We remark, however, that even with the most favorable choice of  $c_1$  the calculated cross sections are significantly smaller than the observed values.

## V. DISCUSSION AND CONCLUSIONS

Our calculations in this article are based on the transition operators derived from a particular version of the chiral effective Lagrangian, the one used in PM<sup>3</sup>K [7]. As mentioned in section II, other choices of the effective Lagrangian are possible, although the main features of our results may be stable against these changes. This point requires further examinations. A related issue is the choice of an explicit form of  $U(x)$  as a function of the pion fields  $\boldsymbol{\pi}(x)$ . Needless to say, if we calculate everything exactly, the results should be independent of particular choices. However, in any practical calculations one needs to expand  $U(x)$  in powers of  $\boldsymbol{\pi}(x)$  and truncate the series, which nullifies the formal equivalence of various choices. Thus, in an approximate calculation such as the present one, the  $pp \rightarrow pp\pi^0$  transition amplitude does depend on the off-shell  $\pi N$  amplitude, which varies when different forms for  $U(x)$  are used. We have employed here a particular form for  $U(x)$ , and the stability of our results against other choices is yet to be studied.

In our calculation, the rescattering transition matrix element corresponding to the  $c_2$ - and  $c_3$ -terms are found to be rather sensitive to the higher momentum components of the nuclear ( $pp$ ) wave function; as a matter of fact, the relevant range of momentum is not much

smaller than the chiral scale  $\Lambda$ . This uncomfortable feature is in fact shared also by other known applications of nuclear  $\chi$ PT, and a satisfactory solution to this problem seems to require the study of terms with higher chiral orders than considered here.

Keeping in mind all the caveats stated above, we still consider it almost certain that, in any reasonably realistic  $\chi$ PT calculations, the rescattering term dominates over the impulse term and their signs are opposite to each other. This implies that the heavy-meson exchange contributions considered in Ref. [4] cannot be invoked as a possible mechanism to enhance  $\sigma_{\text{full}}$  to bring it closer to the observed cross sections. Since it is established that these heavy-meson contributions have the same sign as the impulse term, the addition of these extra contributions to the transition amplitude obtained in the full p-space calculation would result in a destructive interference. Thus the heavy-meson contributions such as considered in Ref. [4] suppresses the cross section instead of enhancing it. Most recently, van Kolck, Miller and Riska [9] considered a yet another diagram involving  $\rho - \omega$  exchanges. Since the sign of this additional contribution is unknown, one way to bring our  $\sigma_{\text{full}}$  closer to the experimental cross sections is to include this new contribution assigning to it the favorable sign. Needless to say, from a  $\chi$ PT point of view, this is a highly *ad hoc* prescription, but it is a possibility.

As mentioned in section II, we have not considered here the loop corrections to the impulse term, corrections that lead to the form factor effect for the impulse vertex. Qualitatively speaking, the inclusion of this effect is expected to reduce the contribution of the impulse term, further enhancing the dominance of the rescattering term. This aspect awaits further study.

We now summarize. For the  $pp \rightarrow pp\pi^0$  reaction near threshold, we have calculated the cross sections, using the effective transition operators derived from chiral perturbation theory ( $\chi$ PT) and employing the *momentum-space representation*. Our p-space calculation is free from the various kinematical approximations that went into the previous  $\chi$ PT calculations [7,8] based on the r-space representation. In what we call *full* p-space calculations, we have retained all the energy-momentum dependence in the transition vertices as dictated

by  $\chi$ PT. The results of the previous r-space calculations are recovered by introducing into the present full p-space calculation the *fixed kinematics approximation*, which consists in freezing the momentum  $\vec{q}$  of the final pion and the energy variable  $k_0$  of the exchanged pion at their values corresponding to the threshold kinematics. The results of the full p-space calculation indicate that the *fixed kinematics approximation* is not justified. Specifically, we have found that in the full p-space calculation the contribution of the rescattering term [Fig. 1(b)] is enhanced by a factor of  $\sim 3$  over the value obtained in the approximate r-space calculations [7,8]. As a result, the rescattering term now dominates over the impulse (Born) term, removing the near complete cancellation between these two terms that existed in the previous calculations. This means that the extremely small cross section reported in Ref. [7,8] becomes much larger in the full p-space calculation [see Fig.4]. The enhancement, however, is not sufficient to explain the observed cross sections. As our work is based on a particular version of the chiral Lagrangian used in Ref. [7], it remains to be seen to what extent the use of other chiral Lagrangians would affect the results. It is also interesting to study whether the remaining discrepancy between the observed and calculated cross sections can be explained in terms of diagrams involving heavy meson exchanges [9]. Thus, the near-threshold  $pp \rightarrow pp\pi^0$  reaction invites further detailed investigations. The principal lesson we draw from the present calculation is that in any serious  $\chi$ PT calculations one must use what is called here the full p-space calculation, avoiding the conventional approximations employed in r-space calculations..

## ACKNOWLEDGMENTS

This work is supported in part by the National Science Foundation, Grant No. PHYS-9602000, by the U.S. Department of Energy, Nuclear Physics Division, Contract No. W-31-109-ENG-38, and by the Grant-in-Aid of Scientific Research, the Ministry of Education, Science and Culture, Japan, Contract No.07640405.

## REFERENCES

- [1] H. O. Meyer *et al.*, Phys. Rev. Lett. **65**, 2846 (1990); Nucl. Phys. **A539**, 633 (1992).
- [2] A. Bondar *et al.*, Phys. Lett. **B356**, 8 (1995).
- [3] G. A. Miller and P. U. Sauer, Phys. Rev. C **44**, R1725 (1991); J.A. Niskanen, Phys. Lett. **B289**, 227 (1992)
- [4] T.-S. H. Lee and D. O. Riska, Phys. Rev. Lett. **70**, 2237 (1993); see also C. J. Horowitz, H. O. Meyer and D. K. Griegel, Phys. Rev. C **49**, 1337 (1994).
- [5] E. Hernández and E. Oset, Phys. Lett. **B350**, 158 (1995).
- [6] C. Hanhart, J. Haidenbauer, A. Reuber, C. Schütz and J. Speth, Phys. Lett. **B358**, 21 (1995).
- [7] B.-Y. Park, F. Myhrer, T. Meissner, J.R. Morones, K. Kubodera, Phys. Rev. **C53**, 1519 (1996).
- [8] T.D. Cohen, J.L. Friar, G.A. Miller and U. van Kolck, Phys. Rev. **C53**, 2661 (1996).
- [9] U. van Kolck, G. A. Miller and D. O. Riska, Phys. Lett. **B388**, 679 (1996).
- [10] D. S. Koltun and A. Reitan, Phys. Rev. **141**, 1413 (1966).
- [11] J. Gasser and H. Leutwyler, Ann. Phys. **158**, 142 (1984).
- [12] For a review, see e.g., V. Bernard, N. Kaiser and Ulf-G. Meissner, Int. J. Mod. Phys. **E4**, 193 (1995)
- [13] E. Jenkins and A. V. Manohar, Phys. Lett. **B255**, 558 (1991).
- [14] S. Weinberg, Phys. Lett. **B251**, 288 (1990); Nucl. Phys. **B363**, 3 (1991); Phys. Lett. **B295**, 114 (1992).
- [15] M. Rho, Phys. Rev. Lett. **66**, 1275 (1991); T.-S. Park, D.-P. Min and M. Rho, Phys. Repts. **233**, 341 (1993); T.-S.Park, I.S. Towner and K. Kubodera, Nucl. Phys. **A 579**,

- 381 (1994); T.-S. Park, D.-P. Min and M. Rho, Phys. Rev. Lett. **74**, 4153 (1995); Nucl. Phys. **A596**, 515 (1996).
- [16] D. Sigg *et al.*, Phys. Rev. Lett. **75**, 3245 (1995).
- [17] E. Jenkins and A.V. Manohar, Phys. Lett. **B259**, 353 (1991); R. Dashen and A.V. Manohar, Phys. Lett. **B315**, 425 (1993); 438 (1993); R. Dashen, E. Jenkins and A.V. Manohar, Phys. Rev. **D 49**, 4713 (1994); H.-B. Tang and P.J. Ellis, Phys. Lett. **B387**, 9 (1996); T.R. Hemmert and B.R. Holstein, preprint hep-ph/9606456 (1996).
- [18] M. Haftel and F. Tabakin, Nucl. Phys. **A158**, 1 (1970).
- [19] R.B. Wiringa, V.G.J. Stoks and R. Schiavilla, Phys. Rev. **C51**, 38 (1995).
- [20] R.V. Reid Jr., Ann. Phys. **50**, 411 (1968)

## FIGURES

FIG. 1. Diagrams contributing to  $pp \rightarrow pp\pi^0$ : impulse term (a) and rescattering term (b). Besides the four-momenta specified in the figures, we use in the text the following notations:  $\vec{p}_i \equiv$  relative momentum between  $\bar{\mathbf{p}}_1$  and  $\bar{\mathbf{p}}_1$ ;  $\vec{p}_f \equiv$  relative momentum between  $\bar{\mathbf{p}}'_1$  and  $\bar{\mathbf{p}}'_2$ ;  $\vec{p} \equiv$  relative momentum between  $\mathbf{p}_1$  and  $\mathbf{p}_2$ .  $\vec{p}' \equiv$  relative momentum between  $\mathbf{p}'_1$  and  $\mathbf{p}'_2$ ;  $W \equiv \bar{p}_{10} + \bar{p}_{20} =$  total energy.

FIG. 2. Total cross sections calculated with the impulse term alone. Solid curve: full p-space calculation; dashed curve:  $\vec{q} = 0$  approximation.

FIG. 3. Total cross sections calculated with the rescattering amplitude alone. Solid curve: full p-space calculation; dash-dotted curve:  $\vec{q} = 0$  approximation; dashes curve: *fixed kinematics approximation*.

FIG. 4. Total cross sections that include both impulse and rescattering amplitudes. Solid curve: full p-space calculation; dash-dotted curve:  $\vec{q} = 0$  approximation; dashed curve:  $\sigma_{\text{fix. kin.}} \times 30$ . The experimental points are from Ref. [1] (open diamonds) and Ref. [2] (solid diamonds).

FIG. 5. Total cross sections obtained in full p-space calculations with the Argonne V18 potential (solid curve), and with the Reid soft-core potential (dashed curve). The experimental points are from Ref. [1] (open diamonds) and Ref. [2] (solid diamonds).

FIG. 6. Total cross sections obtained in full p-space calculations with the parameter set I (solid curve), the parameter set II (dashed curve) and the parameter set III (dash-dotted curve). The experimental points are from Ref. [1] (open diamonds) and Ref. [2] (solid diamonds).



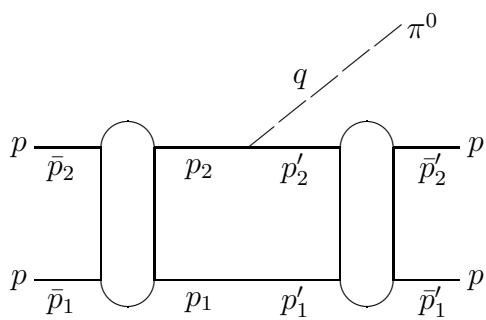


fig. 1(a)

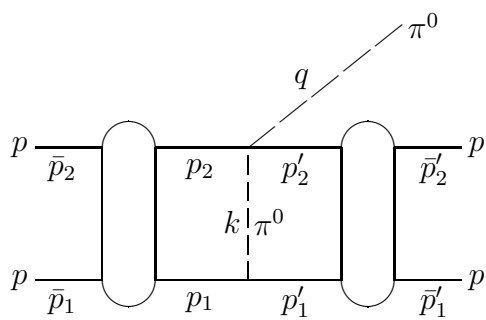


fig. 1(b)

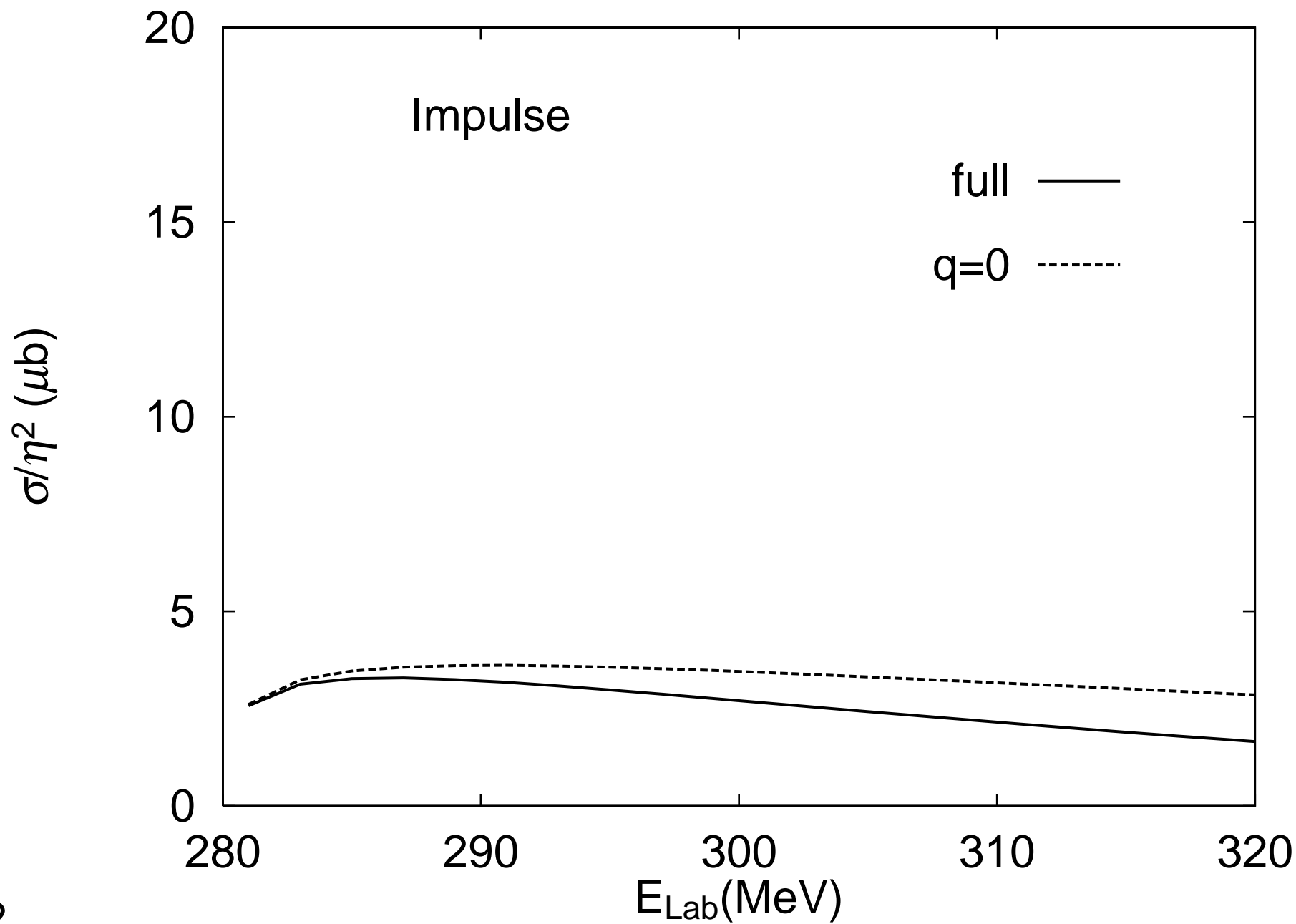


Fig. 2

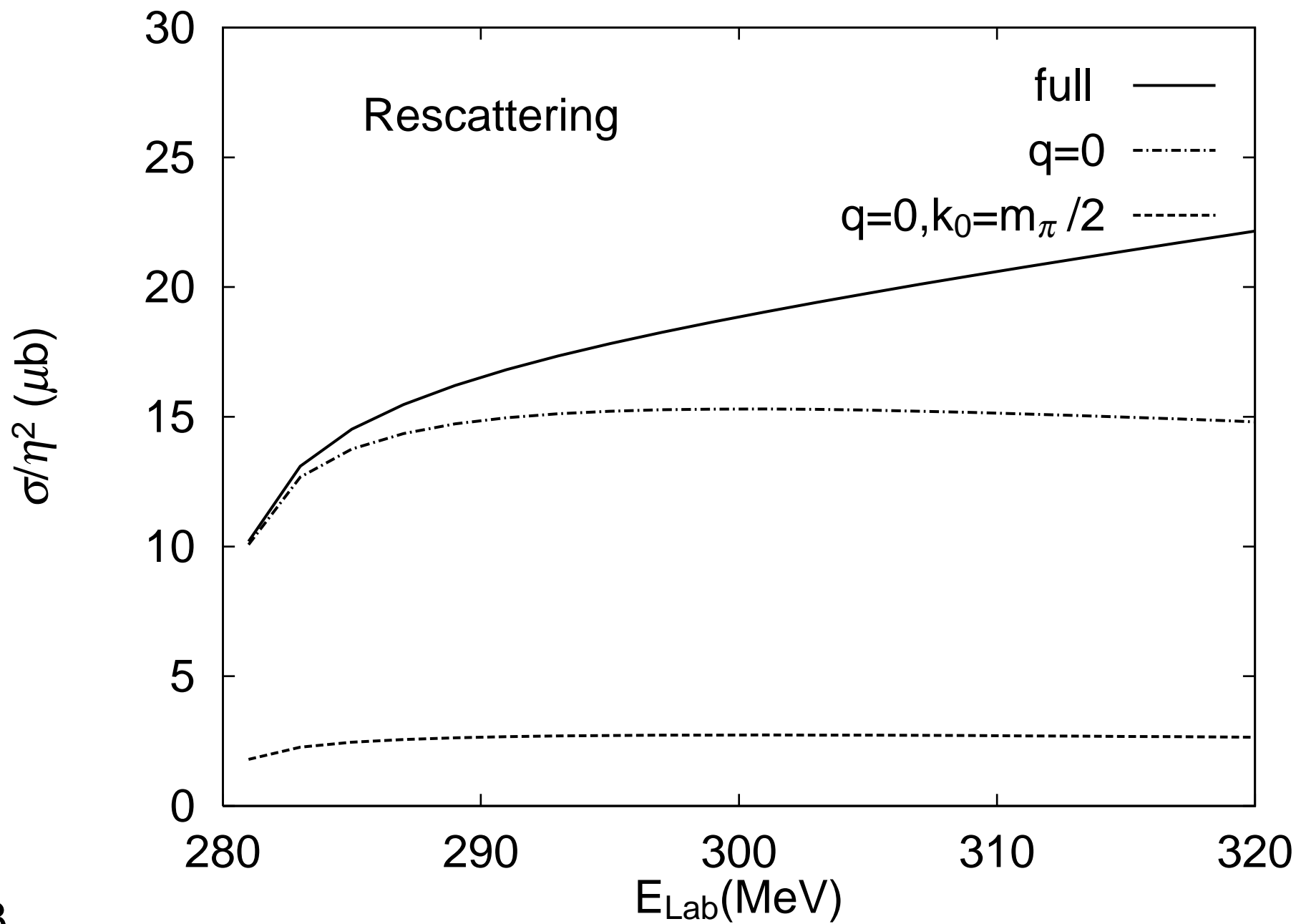


Fig. 3

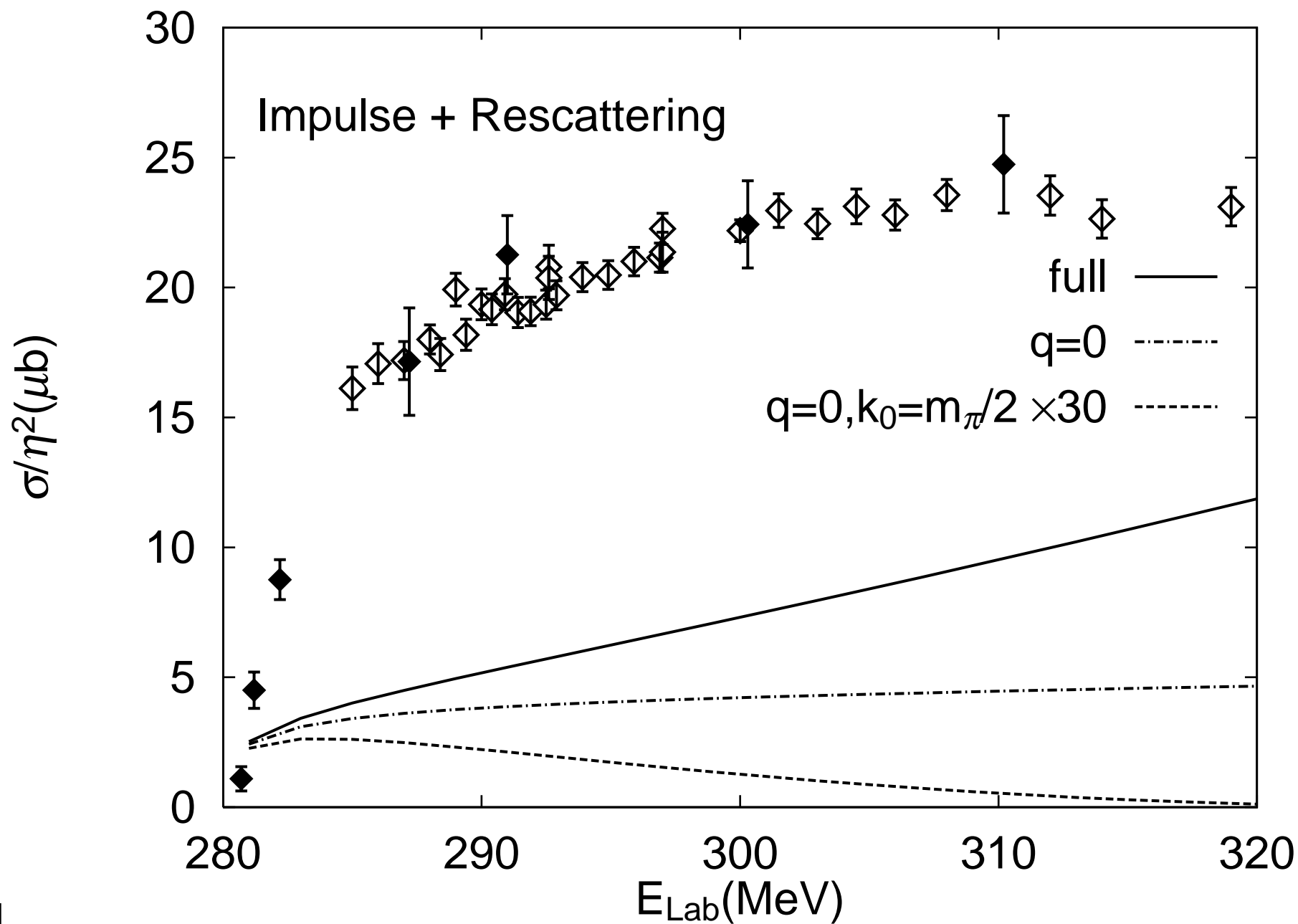


Fig. 4

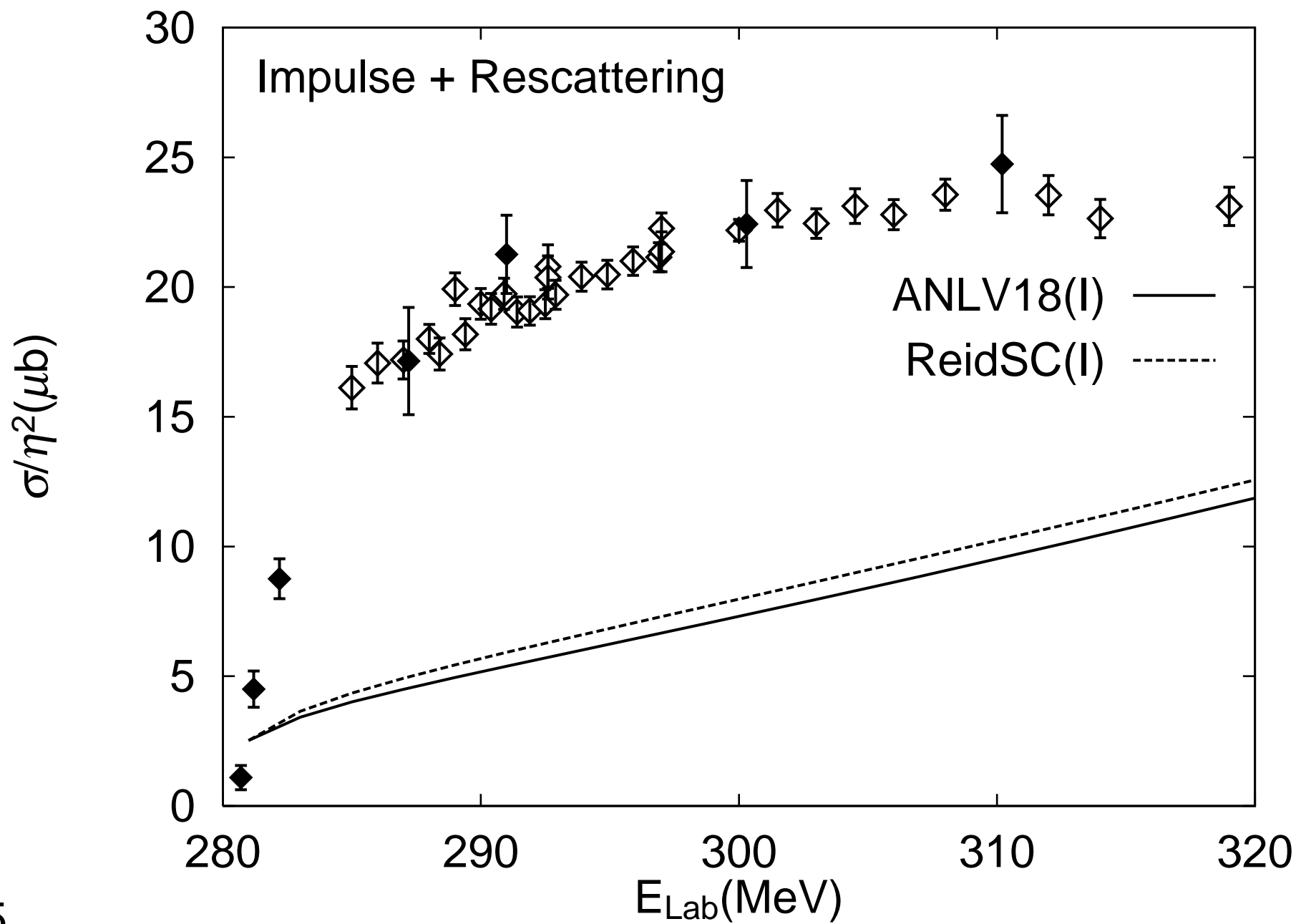


Fig. 5

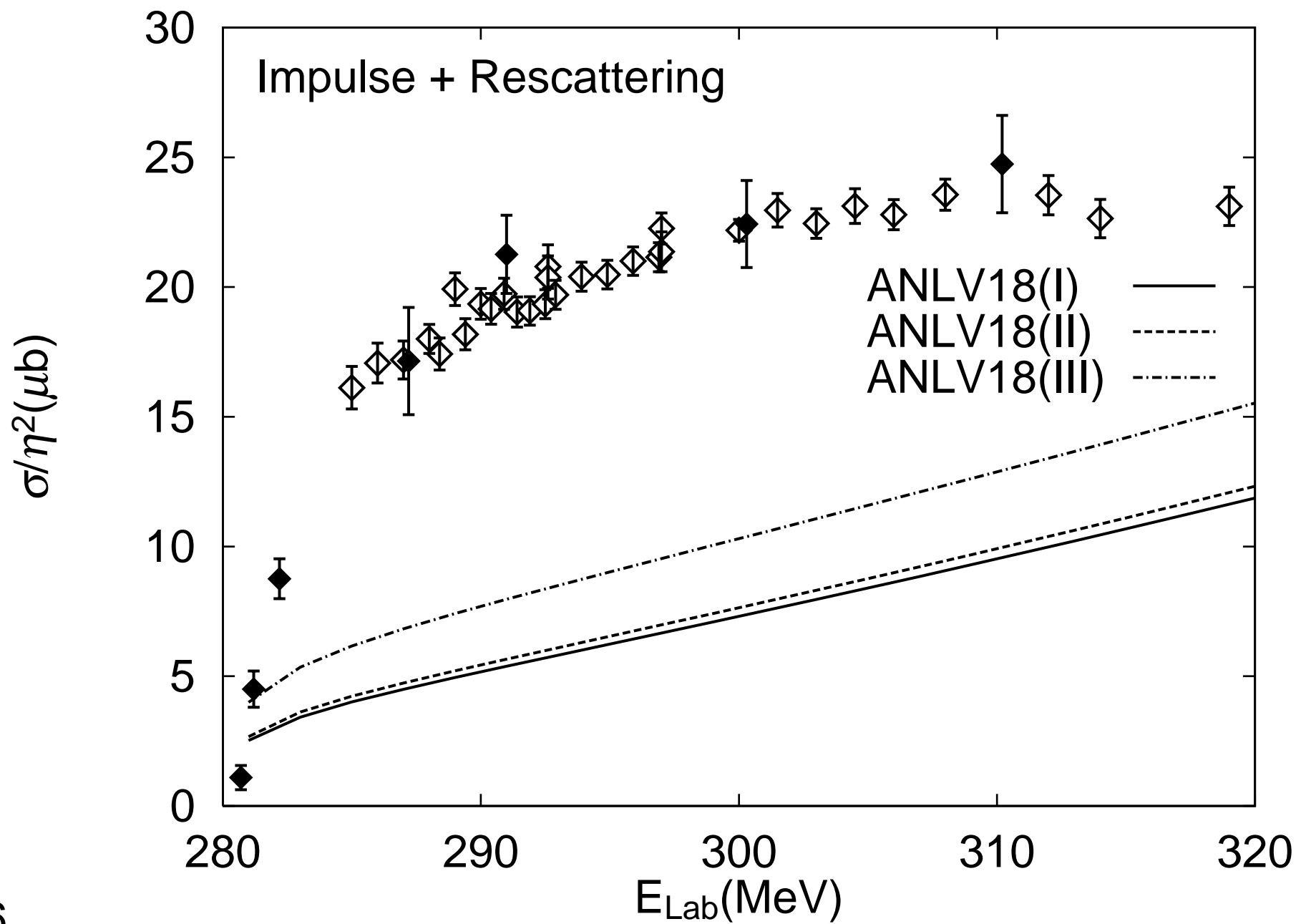


Fig. 6